PAPER www.rsc.org/njc | New Journal of Chemistry

Template controlled synthesis of monometallic zerovalent metal nanoclusters inside cross-linked polymer frameworks: the effect of a single matrix on the size of different metal nanoparticles†‡

Paolo Centomo,*[a] Patrizia Canton,[b] Matteo Ferroni[c] and Marco Zecca[a]

Received (in Montpellier, France) 9th November 2009, Accepted 27th July 2010
DOI: 10.1039/b9nj00648f

Starting from the gel-type, cross-linked copolymer co-poly-{(*N*,*N*-dimethethylacrylamide/4-vinylpyridine/*N*,*N*′-methylenebisacrylamide} (DV44) we prepared nanoclusters of several noble metals (Ru, Rh, Pd, Pt, Ag, Au) inside its polymer framework through the so-called "template-controlled synthesis" approach. This procedure involves the immobilization of the relevant metal centers inside the polymer framework, followed by their reduction to M^0 nanoclusters (in our case, uptake from solutions of suitable precursors and reduction with aqueous solutions of $NaBH_4$, respectively). In this way, a set of monometallic polymer supported nanoclusters (M/DV44, M = Ru, Rh, Pd, Pt, Ag, Au) were obtained. The experimental conditions were set so as to generally obtain a homogeneous radial distribution of the metal throughout the particles of the materials. The latter were characterized by means of transmission electron microscopy for the assessment of the metal nanocluster sizes. The diameter of the nanoclusters generated by reduction inside water-swollen DV44 were compared with the size of the nanopores of the water-swollen polymer framework that had previously been determined by means of inverse steric exclusion chromatography. The diameter of the prevailing pore fractions in water-swollen DV44 was 3.2–4.3 nm and the largest available pores observed had a diameter of 8.1 nm. Nanoclusters with diameters larger than this value were observed in no cases, and in all cases the average diameter of the nanoclusters never exceeded the diameter of the prevailing pore fraction. For Pd/DV44, Ag/DV44 and Au/DV44, the average nanocluster diameter compared very well with the diameter of the prevailing pore fraction.

Introduction

Nanostructured materials are markedly different from both bulk materials and molecular compounds.[1] This stems from the relatively small number of atoms that form the primary nano-sized particles of nanoscale matter. This circumstance implies that the proportion of coordinatively-unsaturated and reactive surface atoms is relatively large. The electronic structure of small primary nanoparticles is featured by pretty narrow bands, which implies a certain degree of electron localization (quantum size effects, Fig. 1).[2] The prospect of new, peculiar properties of nanoscale matter has fostered extensive research in nanoscience and nanotechnology, aimed at the achievement of unprecedented applications, such as the development of novel sensors and catalysts, devices for microelectronics, optical devices, *etc.*[1]

The controlled synthesis of inorganic (metal, oxides, *etc.*) nanoparticles has been in the focus of research for decades.[3] In the case of nanostructured metals, $[Au_{55}(PPh_3)_6Cl_6]$ represents a milestone. Its synthesis on a comparatively large scale was reported by Schmid in 1981:[4] it was so strictly size-controlled that it was possible to formulate it like a molecular compound. Since then, the scope of the bottom-up synthesis of inorganic nanoparticles has been greatly expanded. In the specific field case of metal nanoclusters, research was boosted by interest in these materials as catalysts.[4–6] Soluble, stabilized metal nanoparticles were at first considered as pseudo-homogeneous models of heterogeneous catalysts (micro-heterogeneous catalysts) working under liquid conditions. However, under these conditions, a homogeneous process (catalysis by molecular species detached from the metal nanoclusters) can compete with the micro-heterogeneous process (catalysis over the surface of

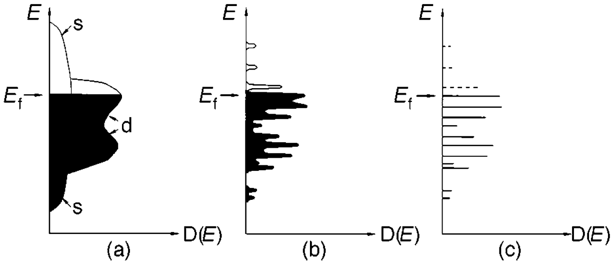

Fig. 1 The electronic situation of bulk metal particles (a) is featured by quasi-delocalized d and s electrons, forming a band structure (b). Electrons form discrete energy levels that are completed in the molecular state by fully localized bonding electrons (c).

---

[a] *Dipartimendo di Scienze Chimiche, Università degli Studi di Padova, Via Marzolo 1, Padova, Italy. E-mail: paolo.centomo@unipd.it; Fax: +39 0498275223; Tel: +39 0498275206*
[b] *Dipartimento di Chimica Fisica, Università degli Studi Ca' Foscari di Venezia, Via Torino 155/b, 30170 Venezia-Mestre, Italy. E-mail: cantonpa@unive.it; Fax: +39 0412346747; Tel: +39 0412346790*
[c] *SENSOR, CNR-INFM, Brescia University, Via Valotti 9, Brescia, Italy. E-mail: matteo.ferroni@ing.unibs.it; Fax: + 39 0303715788; Tel: + 39 0303715749*

† Dedicated to Prof. Benedetto Corain in occasion of his retirement.
‡ Electronic supplementary information (ESI) available: Further SEM and EDX images. See DOI: 10.1039/b9nj00648f

metal nanoclusters).[7,8] On the other hand, metal nanoclusters appear to play a role in several homogeneous catalytic reactions.[9,10]

Heterogeneous metal catalysts can be considered as an insoluble form of stabilized metal nanoclusters. Basically, the support prevents the metal from sintering. From this point of view, it has the same function as the protective agents (ions, ligands, linear polymers) employed in the synthesis of soluble systems. In addition, the importance of metal dispersion, *i.e.* of the small size of metal crystallites (as supported metal particles used to be called), was recognized well before the establishment of nanoscience as an independent field of research. In this sense, heterogeneous catalysis is certainly one of the oldest of the modern nanotechnologies.

Gold represents a recent, dramatic example of the relevance of metal nanocluster size in heterogeneous catalysis. In 1987, Haruta discovered the extraordinary activity of Au^0/TiO_2 catalysts in the low temperature (253 K) oxidation of CO to CO_2 with O_2, in the presence of H, provided the metal nanoclusters are very close to 3 nm in diameter.[11] The preparation of size-controlled heterogeneous metal catalysts is not trivial. Metal nanoclusters are often generated by the reduction of metal precursors after deposition onto the support, either by impregnation or co-precipitation.[12] Under these conditions, the metal nanocluster size is mainly controlled by the concentration of the precursor and its distribution in the support.

If metal nanoclusters are formed inside the micropores of microporous materials, size control can be exerted by the support. In this connection, we have recently shown that it is possible to prepare size-controlled nanostructured metal catalysts supported by gel-type, nanoporous, cross-linked polymers (gel-type resins, GR) (Fig. 2).[13] Gel-type resins are glassy in the dry state, with no appreciable porosity. Nanometer-sized pores and, occasionally, mesopores (a few tens of nanometres in diameter)[14] are formed only when the gel-type resins swell in convenient liquid media. In the swollen state, GRs can incorporate the metal precursor upon either ion exchange or metal coordination. When the swollen metallated resin is treated with a reducing agent, metal nanoclusters are formed inside its nanoporous domains. The size of the metal nanoclusters cannot exceed the size of the internal cavities of the swollen GR,[13] which can be controlled by simply adjusting the degree of cross-linking.[15] Similar effects of the polymer framework on the size of metal nanoclusters generated inside cross-linked polymeric supports matrices were observed by Hanson *et al.*[16] and by Sidorov *et al.*[17] The same level of size control can be achieved with microgels as well, a special class of intramolecularly cross-linked soluble polymers.[18] A similar approach was also applied by Ziolo to the synthesis of nanostructured ferric oxide inside gel-type ion-exchangers ("template-controlled synthesis", TCS).[19] So far, we have investigated the effect of different polymer matrices on only palladium and gold.[13,20] We report in this paper our results concerning the TCS of palladium, platinum, gold, silver, ruthenium and rhodium nanoparticles using a copolymer of *N*,*N*-dimethylacrylamide (92% mol) and 4-vinylpyridine (4% mol), cross-linked with *N*,*N*′-methylenebisacrylamide (4% mol).

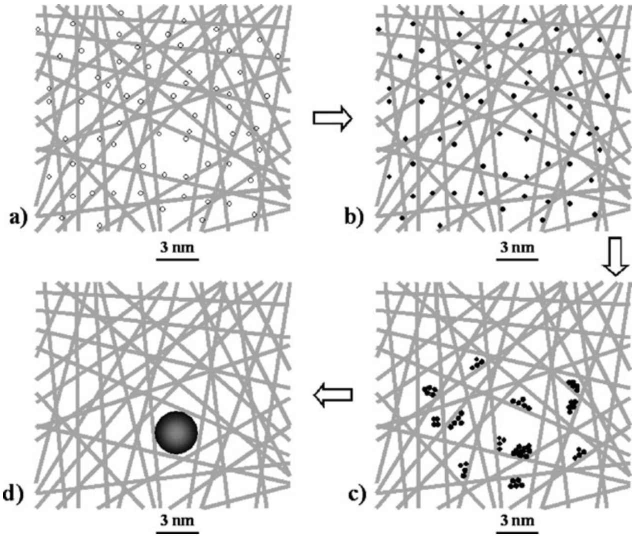

Fig. 2 Model for the generation of size-controlled metal nanoparticles inside metallated resins: (a) Pd^{II} is homogeneously dispersed inside the polymer framework; (b) Pd^{II} is reduced to Pd^0; (c) Pd^0 atoms start to aggregate in metal seeds; (d) a single 3 nm nanocluster is formed and embedded inside the largest mesh present in the surrounding fraction of the polymer framework.

Results and discussion

The ability of polymer frameworks to restrict the size of metal nanoclusters generated in their interior has been observed by different authors[13,16,17,20] under quite different conditions and is likely to be a general phenomenon. However, although the first relevant observations date back to 1974,[16] no systematic investigation on the relationship between the size of the metal nanoclusters and the morphology of the polymer framework where they are generated has been undertaken so far. To show that TCS of metal nanoparticles inside cross-linked polymeric matrices can be a general approach to the preparation of nanoclusters of different metals, we have investigated the templating ability of a single cross-linked polymer matrix in the generation of metal nanoclusters of different metals. In particular, we have taken into account co-poly-{(*N*,*N*-dimethethylacrylamide/4-vinylpyridine/*N*,*N*′-methylenebisacrylamide} (DV44), which has been already used in previous studies in our laboratories, for the preparation of polymer-supported nanoparticles of ruthenium, rhodium, palladium, platinum, silver and gold. DV44 is a gel-type functional co-polymer containing 4% (mol mol^{-1}) 4-vinylpyridine (VP) units and 4% (mol mol^{-1}) cross-linked with *N*,*N*′- methylenebisacrylamide (MBAA). The remainder of the polymer structure (Scheme 1) is formed of *N*,*N*-dimethethylacrylamide (DMAA). The co-monomers are miscible in the indicated proportions, and accordingly DV44 could be obtained by γ-ray (^{60}Co) initiated mass polymerization.

Dry DV44 was characterized by scanning electron microscopy (SEM), which showed it to be compact, of glassy morphology and with the absence of micrometre-sized pores that are typical of gel-type cross-linked co-polymers (Fig. 3).

The morphology of the co-polymer in the dry state, however, is hardly relevant to the conditions of TCS of metal nanoclusters inside the polymer framework. In fact, the nanoclusters are generated upon reduction of metal precursors taken up by the

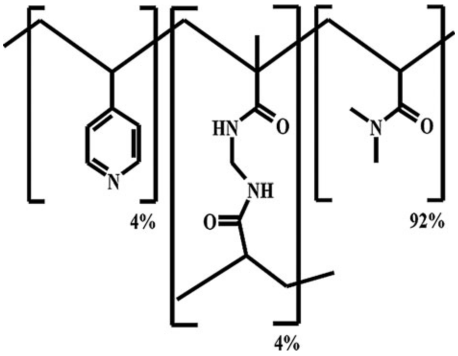

Scheme 1 Chemical structure of the DV44 resin.

solid support from suitable solutions, *i.e.* under liquid–solid conditions. Gel-type cross-linked copolymers have, in general, relatively low cross-linking degrees (less than 8%, mol mol^{-1})[14] and swell to some extent when they are in contact with a liquid medium. If the affinity of the polymer matrix to the liquid is high, the volume of the former can even increase several times upon swelling. The most straightforward way to introduce metal precursors into the polymer framework is to treat the polymeric material with a solution of a metal compound that can be taken up by the support. A direct chemical interaction, such as metal coordination of polymer-bound functional groups or ion exchange, provides a strong driving force for the process. In the case of gel-type cross-linked co-polymers, which are usually characterised by low specific surface areas in the dry state, the process is also facilitated by a high swelling degree of the support in the metal solution employed.

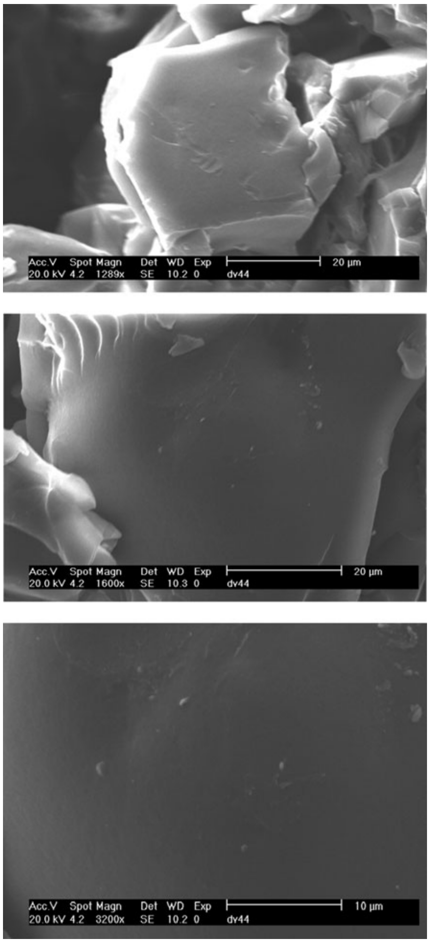

Fig. 3 Secondary electron SEM images of dry DV44 resin at different magnifications.

The morphology of cross-linked polymers in the swollen state can be conveniently assessed by inverse steric exclusion chromatography (ISEC),[21] a chromatographic technique where the swollen polymer to be characterized is employed as the stationary phase in measurements of elution volumes of standard solutes of different and known effective molecular size. In many cases, specific (enthalpic) interactions between solute molecules and the investigated column can be made negligible by the suitable selection of experimental conditions, under which the elution behavior of the solutes is predominantly driven by the morphology of the pore system of the swollen material.

Morphological information can be extracted from the elution volume values of discrete sets of sets of standard solutes by means of a mathematical analysis based on Ogston's model,[22] which depicts pores as void spaces among randomly-oriented rigid rods representing polymer chains. The pore size in Ogston's model is characterized by the concentration of the cylindrical rods expressed in units of length per unit volume (typically nm nm^{-3}). This intensive parameter is qualitatively equivalent to the pore diameter of a more conventional cylindrical pore model. Although Ogston's analysis model is recommended[21b,23] for describing the porosity of swollen polymeric materials (it is closer to the physical reality), simple models that depict the real morphology of a swollen polymer framework as a set of discrete fractions, each consisting of singly-sized, geometrically regular pores, can serve just as well.[21a] Hence, the analysis of ISEC chromatographic data using the cylindrical pore concept is perfectly acceptable from a mathematical point of view.[21b] It provides a description of the morphology of swollen polymers similar to that obtained from Ogston's model, where the polymer chain concentration is replaced by the pore diameter, the physical meaning of which is more immediately grasped. The cylindrical pore model does not provide a reliable estimate of the extensive parameters (the volume of the single pore fractions),[21c] but this is not relevant for the purpose of the present discussion, and the morphology of water-swollen DV44 will be presented in this form.

The ISEC characterization of DV44 shows that no macroporous portions of the polymer mass are present (Table 1), in agreement with SEM observations. The estimated pore diameters are less than 10 nm, the highest value being 8.1 nm.

As the distribution of pore fraction volumes cannot be employed for quantitative comparisons, we do not know whether the most abundant pore fraction is the 3.2 or the 4.3 nm one. In spite of this, the difference between the volumes of these two fractions from those of the others is such that we can safely state that the diameter of almost all the nanopores in water-swollen DV44 is included within the 3–4.5 nm range.

Details of the experimental conditions applied to the preparation of nanoclusters of several noble metals (Ru, Rh, Pd, Pt, Ag, Au) inside DV44, along with the observed weight metal percentage and the average nanocluster diameter, are reported in Table 2. The solvent for the metal uptake was chosen according to the solubility of the metal precursor. In each

Table 1 ISEC characterization of water-swollen DV44

Pore diameter/nm	Fraction volume/$cm^3\ g^{-1}$	Specific surface area/$m^2\ g^{-1}$
0.6	0.331	2208.4
1.1	0.000	0.0
1.6	0.000	0.0
2.7	0.000	0.0
3.2	1.373	1715.9
4.3	1.192	1118.5
8.1	0.089	44.2
30.9	0.000	0.0
ΣV_i	2.985	
V_{gel}	2.67	

case, the amount of metal precursor put in contact with DV44 was such so as to provide a final 1% (w/w) metal percentage in case of complete metal uptake. The data in Table 2 show that there is no relationship between the final metal percentage and the nature of the solvent employed in this step. This indicates that poor swelling is not likely to be the cause of the low incorporation of silver, rhodium and ruthenium. At the moment, the reason is not clear as to why these metals were taken up to such a low extent. What is important, however, is that the reduction of the metal centers dispersed within the polymer framework of DV44 was carried out with aqueous solutions of $NaBH_4$ for all the samples. This implies that the morphology of the polymer framework in the crucial step of generating metal nanoclusters was the same as described by the ISEC analysis, and that the comparison between the size of the metal nanoclusters and the pore diameters makes sense.

According to our experience with water swellable polymer matrices (such as *N*,*N*-dimethylacrylamide-based resins),[15c,20,24] $NaBH_4$ was used in large excess to favor a homogeneous radial distribution of the metal nanoclusters across the polymer particles.

The different M/DV44 materials were analyzed by means of SEM and energy dispersive x-ray spectroscopy (EDX, see the ESI‡; as an example, Au characterization is reported in Fig. 4). It turns out that the elemental mapping resembles the surface morphology of the sample, suggesting that the metal distribution is homogeneous. This demonstrates that the metal uptake involved the whole swollen polymer framework, *i.e.* the latter was swollen enough in the employed solvents and that the metal did not migrate towards the particle edges during the reduction step owing to the high proportion of reducing agent employed.[25] The most remarkable exception is Ru/DV44, where the metal distribution is clearly "egg"-like, but this is likely to be a consequence of the extremely low content of metal in the material (close to the detection limits of AES-ICP).

As a matter of fact, rhodium, which was taken up from the same solvent (equal swelling degree of DV44) and to a larger (albeit low) extent was much more homogeneously distributed than ruthenium.

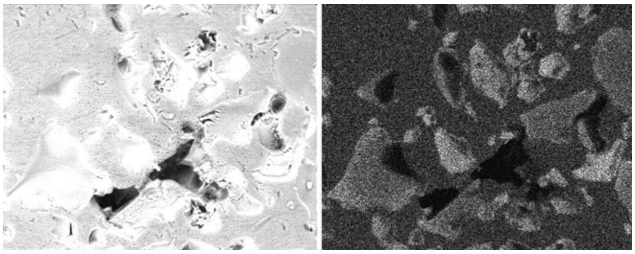

Fig. 4 SEM and EDX images for Au/DV44 (see the ESI for characterization of the M/DV44 materials, M = Ru, Rh, Ag, Pd, Pt, Au‡).

The samples were finally characterized by transmission electron microscopy (TEM). To ensure a reliable assessment of the metal nanoparticle size, each sample was analyzed the day after its preparation. Representative TEM images of the M/DV44 materials and the respective nanocluster size distributions are reported in Fig. 5.

Nanoclusters larger than the widest available pores were observed in no cases: only Ag and Au formed a very small fraction of nanoparticles of about 8 nm in diameter, which is comparable to the 8.1 nm diameter of the largest pores found in water-swollen DV44. Interestingly, the average diameters of the Pd, Ag and Au nanoclusters were almost coincident with the diameter of the prevailing pores of water-swollen DV44, as determined by ISEC analysis. This suggests that the templating polymer framework acts as a relatively rigid "mold" that prevents the formed metal nanoclusters growing larger than the pores. Therefore, these results give further support to the hypothesis that steric control is predominant in the TCS of nanoparticles within polymer frameworks, as already proposed in the literature.[13,17]

For Ru, Rh and Pt, the average diameter is lower than the diameter of the pores of the swollen polymer matrix. This is

Table 2 Selected data on the preparation and characterization of Ru, Rh, Pd, Pt, Ag and Au nanoclusters generated inside DV44 (M/DV44)[a]

Material	Metal precursor	Solvent	$\%_{metal}$ (w/w)[b]	Average diameter/nm[c]
DV44/Pt	$[Pt(NCCH_3)_2Cl_2]$	CH_3CN	0.88	2.4
DV44/Pd	$Na_2[PdCl_4]$	H_2O	0.88	4.4
DV44/Au	$HAuCl_4 \cdot xH_2O$	CH_3CN	0.64	3.5
DV44/Ag	$AgNO_3$	H_2O	0.09	4.2
DV44/Rh	$[Rh_2(OAc)_4]$	EtOH	0.03	1.9
DV44/Ru	$RuCl_3 \cdot xH_2O$	EtOH	< 0.01	2.0

[a] The reduction of the anchored metal precursors was performed upon tratment with aqueous solutions of $NaBH_4$. [b] AES-ICP analysis. [c] TEM.

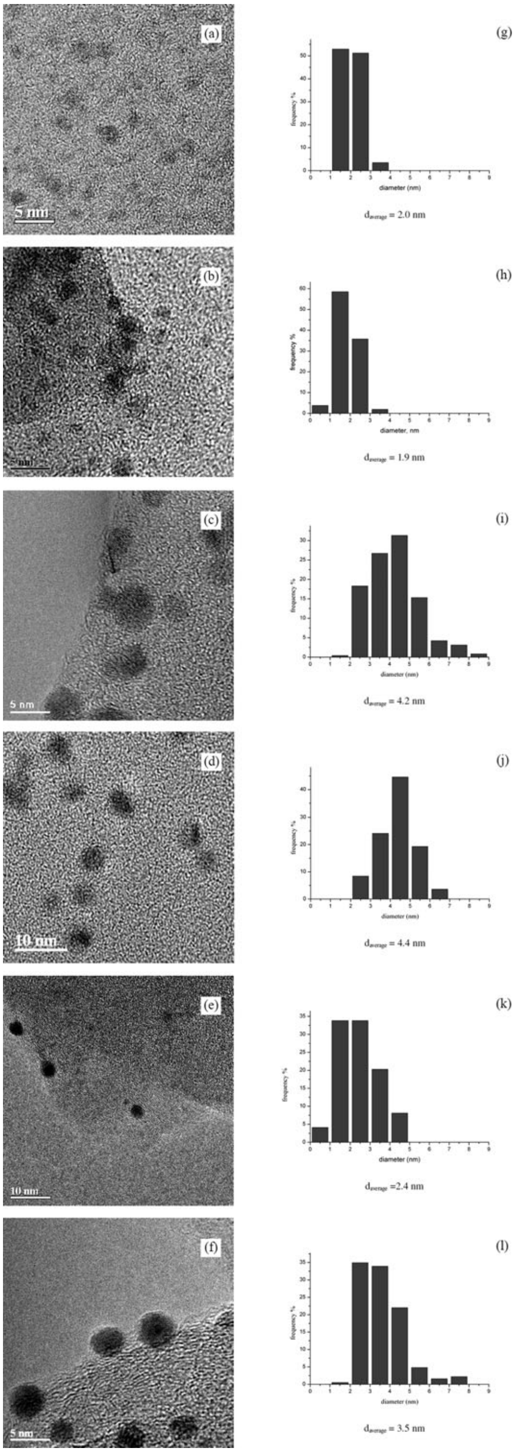

Fig. 5 Representative TEM images (a–f) of M/DV44 and size distribution (g–l) of M^0 nanoparticles (a, g: Ru; b, h: Rh; c, i: Ag; d, j: Pd; e, k: Pt; f, l: Au).

the first time that we have observed the formation of nanoclusters smaller than the pores available for their generation in a swollen polymer matrix. The reasons for this "undersizing" of the metal nanoclusters in comparison to the dimensions of the cavities of the underlying templating polymer framework are not clear at the moment. This could be due to intrinsic properties of the nanoclusters or to stabilization of small particles through some specific (non-steric) interactions (something similar to capping in nanoparticles stabilized by linear, soluble polymers) or even be due to kinetic reasons. In the case of Ru/DV44 and Rh/DV44, the small nanocluster size could be a consequence of the small amount of metal in the materials.[25]

Altogether, these new results are in agreement with the simple model of the growth of metal nanoparticles inside a templating polymer framework, as proposed in Fig. 1. According to this model, the TCS effect is due to the steric constraints of the relatively rigid polymer framework. This property makes cross-linked polymers a general class of very interesting and useful supports for the easy preparation of heterogeneous, nanostructured metal catalysts with a predictable size of metal nanocluster.

Experimental

Materials and apparatus

All reagents and solvents (reagent grade) were obtained from various commercial sources and used as received. SEM analyses were carried out on a Cambridge Stereoscan 250, equipped with EDX 9800. Transmission electron micrographs were taken with a JEOL 2010 with GIF. Thermogravimetric analysis was carried out with a Perkin Elmer TG-2 themobalance. Elemental analysis for C, H, N was carried out with a Carlo Erba 3300 analyzer. TEM analysis was carried out with a JEM 3010 (JEOL) electron microscope operating at 300 kV, point to point resolution at Scherzer defocus of 0.17 nm.

Synthesis of DV44 resin

In a typical experiment, DMAA (10.77 g), VP (0.50 g), and MBAA (0.73 g) were mixed in a cylindrical glass vessel to give a clear colorless solution that, after oxygen removal by means of nitrogen bubbling, was subjected to γ-irradiation (^{60}Co) for 18 h, at a distance of 17.1 cm from the source (total dose was *ca.* 10 KGy) at room temperature. The solution was transformed into a transparent pale yellow cylindrical block that underwent extensive fragmentation due to the swelling in water (72 h). The resin was fully ground with an IKAA10 impact grinder and washed for 96 h with methanol under reflux with Soxhlet apparatus. The polymer material was dried at 60 °C under approximately 6 mmHg pressure and finally sieved to 180 – 400 μm. Elemental analysis: expected% (experimental): C, 61.90 (59.25); H, 5.34 (8.56); N, 15.07 (13.30).

Metalation of DV44 composites

1.2 g of DV44 was swollen in 50 ml of the required liquid (Table 3) and kept for 2 h under moderate mechanical stirring (swirling plate). In the case of Pd^{II} loading, $PdCl_2$ and 30 mg of NaCl was added to 40 ml of water. The resulting suspension was refluxed under magnetic stirring until complete solid dissolution (yellow solution). Then, 10 ml of the metal precursor solution (Table 1) were added to the suspension and kept under moderate stirring at r.t. The metallated samples were recovered upon filtration, washed with the respective solvent and dried in vacuum at 60 °C to constant weight.

Table 3 Experimental conditions and metal elemental analysis for the DV44 supported metal samples

Sample	Cluster precursor	Weight/mg	Solvent	$\%_{metal}$ (w/w)
Ag/DV44	$AgNO_3$	18.9	H_2O	0.09
Au/DV44	$HAuCl_4$	20.7	CH_3CN	0.64
Pd/DV44	$PdCl_2$	21.7	H_2O	0.88
Pt/DV44	$Pt(NCCH_3)_2Cl_2$	21.4	CH_3CN	0.88
Ru/DV44	$RuCl_3$	24.6	EtOH	< 0.01
Rh/DV44	$Rh(OAc)_2$	32.6	EtOH	0.03

Reduction of the metallated composites to M/DV44 (M = Ag, Au, Pd, Pt, Ru, Rh)

The metallated composite to be reduced (*ca.* 1 g) was suspended in *ca.* 50 ml water and left under moderate stirring for 2 h. Then, 10 ml of an aqueous solution of $NaBH_4$ (250 mg) was added to the suspension. The mixture was stirred manually until the initial vigorous effervescence subsided, and left under moderate mechanical stirring until the liquid phase turned colorless (*ca.* 60 min). The solid was finally filtered, washed with water and dried to constant weight at 60 °C in vacuum.

Preparation of samples for TEM analysis

A few milligrams of the powdered samples were mixed with high purity isopropyl alcohol. The suspension was sonicated for 5 min in order to disrupt possible agglomerates. A 5 μl droplet of suspension was transferred onto an amorphous carbon film and then put into the microscope.

Preparation of samples for SEM-EDX analysis

A few milligrams of each sample were embedded inside a drop of epoxy-resin (Araldite 2020 A/B) on the surface of a microscope slide. The resin was left to harden in an oven at 40 °C for 24 h. The upper part of the specimen was cut in order to show cross-sections of the embedded particles. The surface was lapped with rubbing paper sheets soaked with an alcoholic suspension of diamond powder and fixed rotating plates. A thin layer of carbon was finally deposited on the surface.

Conclusions

We have compared the effects of a single polymer framework in the TSC of different metal nanoclusters inside the gel-type, cross-linked polymer DV44 for the first time.

The results fully confirm the ability of the polymer framework to control to a very good extent the size of the metal nanoclusters generated in water-swollen DV44. The observed size of the metal nanoclusters never exceeds the size of the pores of DV44, assessed not in the dry state but in the working state (water-swollen) by means of ISEC nanomorphological analysis. In many cases, the average nanocluster size strictly compares with the diameter of the prevailing pores within the swollen polymer framework. Altogether, the results highlight the mainly steric nature of the templating effect of the polymer framework in the TCS of nanoclusters.

Acknowledgements

Dr Karel Jeřábek (Academy of Science of the Czech Republic—Institute of Chemical Process Fundamentals, Prague) and Dr Paolo Guerriero (Institute of Inorganic Chemistry and Surfaces, ICIS-CNR, Padova) are gratefully acknowledged for ISEC and SEM-EDX measurements, respectively. We are grateful to Mr Tiziano Finotto for his skilled technical assistance.

References

1 S. C. Tjong and H. Chen, *Mater. Sci. Eng., R*, 2004, **45**, 1.
2 G. Schmid, *J. Chem. Soc., Dalton Trans.*, 1998, **7**, 1078.
3 *Metal Nanoclusters in Catalysis and Material Science: The Issue of Size Control*, ed. B. Corain, G. Schmid and N. Toshima, Elsevier, Amsterdam, 2008 (ISBN: 978-0-444-53057-8).
4 G. Schmid, R. Pfeil, R. Boese, F. Brandermann, S. Meyer, G. H. M. Calis and J. W. A. Van der Velden, *Chem. Ber.*, 1981, **114**, 3634.
5 J. D. Aiken III and R. G. Finke, *J. Mol. Catal. A: Chem.*, 1999, **145**, 1.
6 A. Roucoux, J. Schulz and H. Patin, *Chem. Rev.*, 2002, **102**, 3757.
7 R. A. Sheldon, M. Wallau, I. W. C. E. Arends and U. Schuchardt, *Acc. Chem. Res.*, 1998, **31**, 485.
8 J. A. Widegren and R. G. Finke, *J. Mol. Catal. A: Chem.*, 2003, **198**, 317.
9 C. M. Hagen, J. A. Widegren, P. M. Maitlis and R. G. Finke, *J. Am. Chem. Soc.*, 2005, **127**, 4423.
10 E. E. Finney and R. G. Finke, *Inorg. Chim. Acta*, 2006, **359**, 2879.
11 M. Haruta, in *Metal Nanoclusters in Catalysis and Material Science: The Issue of Size Control*, ed. B. Corain, G. Schmid and N. Toshima, Elsevier, Amsterdam, 2008, pp. 183–199 (ISBN: 978-0-444-53057-8).
12 C. H. Satterfield, in *Heterogeneous Catalysis in Industrial Practice*, McGraw-Hill, New York, 2nd edn, 1991.
13 B. Corain, K. Jeřábek, P. Centomo and P. Canton, *Angew. Chem., Int. Ed.*, 2004, **43**, 959.
14 A. Guyot, in *Synthesis and Separations Using Functional Polymers*, ed. D. C. Sherrington and P. Hodge, John Wiley, New York, 1988, pp. 1.
15 (*a*) A. Biffis, B. Corain, M. Zecca, C. Corvaja and K. Jeřábek, *J. Am. Chem. Soc.*, 1995, **117**, 1603; (*b*) A. A. D'Archivio, L. Galantini, A. Panatta, E. Tettamanti and B. Corain, *J. Phys. Chem. B*, 1998, **102**, 6779; (*c*) C. Burato, P. Centomo, G. Pace, M. Favaro, L. Prati and B. Corain, *J. Mol. Catal. A: Chem.*, 2005, **238**, 26.
16 D. L. Hanson, J. R. Katzer, B. C. Gates, G. C. A. Schuit and H. F. Harnsberger, *J. Catal.*, 1974, **32**, 204.
17 S. N. Sidorov, I. V. Volkov, V. A. Davankov, M. P. Tsyurupa, P. M. Valetsky, L. M. Bronstein, R. Karlinsey, J. W. Zwanziger, V. G. Matveeva, E. M. Sulman, N. V. Lakina, E. A. Wilder and R. J. Spontak, *J. Am. Chem. Soc.*, 2001, **123**, 10502.
18 A. Biffis, N. Orlandi and B. Corain, *Adv. Mater.*, 2003, **15**, 1551.
19 R. F. Ziolo, E. P. Giannelis, B. A. Weinstein, M. P. O'Horo, B. N. Ganguly, V. Mehrotra, M. W. Russell and D. R. Huffman, *Science*, 1992, **257**, 219.
20 B. Corain, C. Burato, P. Centomo, S. Lora, W. Meyer-Zaika and G. Schmid, *J. Mol. Catal. A: Chem.*, 2005, **225**, 189.
21 (*a*) K. Jeřábek, *Anal. Chem.*, 1985, **57**, 1595; (*b*) K. Jeřábek, *Anal. Chem.*, 1985, **57**, 1598; (*c*) K. Jeřábek, in *Cross Evaluation of Strategies in Size-Exclusion Chromatography*, ed. M. Potschka and P. L. Dubin, ACS Symp. Ser. 635, American Chemical Society, Washington DC, USA, 1996, pp. 211.
22 A. G. Ogston, *Trans. Faraday Soc.*, 1958, **54**, 1754.
23 J. C. Laurent and J. Killander, *J. Chromatogr., A*, 1964, **14**, 303.
24 M. Zecca, P. Centomo and B. Corain, in *Metal Nanoclusters in Catalysis and Material Science: The Issue of Size Control*, ed. B. Corain, G. Schmid and N. Toshima, Elsevier, Amsterdam, 2008, pp. 201–232 (ISBN: 978-0-444-53057-8).
25 C. Besson, E. E. Finney and R. G. Finke, *Chem. Mater.*, 2005, **17**, 4925.